MATERIAL MODEL FOR SIMULATING STRAIN-HARDENING CEMENTITIOUS COMPOSITES IN LS-DYNA

Ravi Ranade and Victor C. Li

Dept. of Civil and Environmental Engineering, University of Michigan Ann Arbor, USA

Abstract

While there are a few material models available in LS-Dyna for simulating concrete and strain-softening fiber-reinforced concretes (FRC) under dynamic loads, there is currently no material model that explicitly simulates the inelastic behaviour of Strain-Hardening Cementitious Composites (SHCC). This creates a bottleneck for the implementation of SHCCs in the structures subjected to dynamic loads such as impacts and blasts. In this research, one of the material models originally developed for strain-softening concretes in LS-Dyna, MAT_072R3, is used to simulate an ultra-high strength SHCC in slabs under moderate velocity impacts. This is accomplished by taking advantage of the two separate damage evolution parameters in tension and compression (in spite of only one damage function) in the MAT_072R3 model, and by raising the built-in tensile pressure cutoff. An understanding of the MAT_072R3 material model (its relevant input parameters) from the perspective of a user wanting to simulate the strain-hardening behaviour of SHCC is presented in this paper.

1.   INTRODUCTION

Structural analysis using finite element (FE) method plays a key role in the design and response prediction of almost all modern structures, particularly those subjected to complex loading. Appropriate material models are, therefore, needed to simulate the behaviour of SHCC in the FE analyses.

Simulating the behaviour of SHCC in FE analysis presents certain unique challenges. SHCC, similar to other cementitious materials, are highly complex and heterogeneous materials with significant local variation of properties. These variations in properties at macro-scale are particularly apparent at the sites of cracking in SHCC. Furthermore, SHCC have significantly different behaviour in compression than in tension, and their behaviour under multi-axial loading is different than under uniaxial loading. These complexities of SHCC behaviour are typically addressed using concrete plasticity theory with three-dimensional failure surface [1].

Recognizing the importance of developing an FE material model for SHCC, significant efforts have been made in this direction by Kabele [2], van Zijl [3], Dick-Neilsen [4], Maekawa [5], and many others. A systemic review of these models is presented in a recent RILEM State-of-the-art report [6]. Although these efforts have been successful in modelling the behaviour of SHCC under quasi-static loading with specialized softwares, there remains a need to develop an FE material model, for simulating the behaviour of SHCC under highly dynamic loads, that is implementable in a widely used commercial software such as LS-Dyna to realize the true potential of SHCC's unique properties in advanced structural applications.

The objective of this study is to investigate the feasibility of simulating the behaviour of an ultra-high strength SHCC under dynamic loads in LS-Dyna using one of the existing models (MAT_072R3) in its material library. For this purpose, appropriate input parameters are determined for the LS-Dyna material model based on the available experimental data on SHCC's material properties. The structural response of an SHCC slab under drop-weight impact is then computed using FE analysis and compared with the results of the drop-weight experiments on thin SHCC slabs to verify the effectiveness of the LS-Dyna material model.

2.   MODELED PROBLEM

A schematic sketch of the drop-weight experiment is shown in Figure 1(a). A constant weight of 16 kg is dropped onto thin SHCC slabs (area of 305 x 305 mm^2 and height of 25.4 mm) using a cylindrical steel impact head of diameter 76.2 mm from three different heights with corresponding impact velocities of 2.30 m/s, 3.25 m/s, and 4.60 m/s. The SHCC slab specimen is simply placed on the hollow steel support that is 25.4 mm wide running continuously along all four edges of the slab as shown in Figure 1(b). Load and acceleration time-histories are recorded using a dynamic load cell and two accelerometers, respectively. The acceleration-time histories are time-integrated twice (in post-processing) to determine the displacement-time histories for comparison with the LS-Dyna model results.

3.   LS-DYNA MODEL PARAMETERS

The FE analysis in this research was performed using the commercially available software LS-Dyna with Lagrangian mesh formulation and explicit time integration. This section describes all model parameters except for the SHCC that are described in Section 4.

3.1   Geometry and Meshing

The FE model of the drop-weight test is shown in Figure 2. Due to the symmetry of the problem about two orthogonal axes, only a quarter of the square slab is modeled with appropriate boundary conditions (Section 3.3). Meshing of the slab in LS-Dyna is performed using 8-node constant stress solid (brick) elements with one-point integration. The stiffness form of the Flanagan-Belytschko hourglass control method is activated in LS-Dyna to avoid zero-energy modes, which may form due to the reduced integration. Such hexahedral mesh elements have been satisfactorily used in dynamic models of concrete structures [7,8,9].

The size of the brick element for modeling the SHCC slab as determined from a mesh convergence study is 2x2x2 mm^3. Similar to the slab, the impact head and the base support are also discretized using brick elements, although with different material (steel). Element sizes close to that used for modelling the SHCC slab elements are used to model the impact

head and the support, as it is advisable to have the mesh density of contacting surfaces similar
to each other for faster numerical convergence.
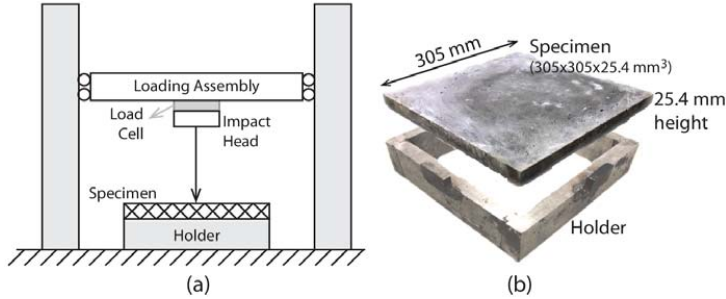
Figure 1: Drop weight impact experiment
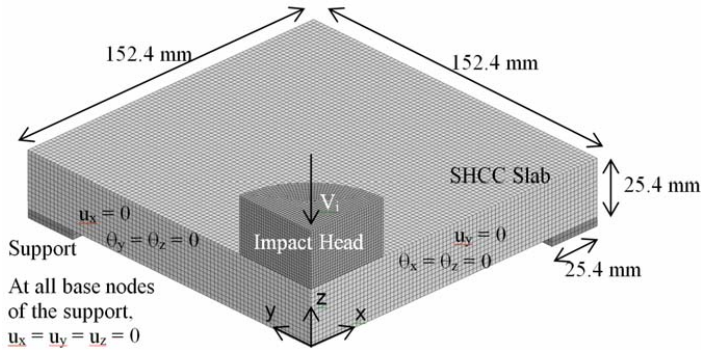
Figure 2: FE Model of the Drop-weight Test

3.2 Material Model for Impact Head and Support

The impact head and the base support, physically made of 4140 steel, are modeled using
the LS-Dyna material model MAT_003 that is typically used for modeling steel and other
metals exhibiting isotropic behaviour with plasticity and rate effects. The Young's modulus,
Poisson ratio, yield stress, and tangent modulus are set equal to 200 GPa, 0.30, 415 MPa, and
0 GPa (assuming elastic perfectly plastic), which are the typical properties used for the 4140
steel. Although the density of 4140 steel is about 7800 kg/m^3, it is set equal to 138129 kg/m^3
to concentrate the entire mass (16 kg) of the loading assembly in the modeled impact head (a
cylinder of height 25.4 mm and diameter 76.2 mm), thereby preserving the kinetic energy of
impact. The effect of strain rate in steel is captured through Cowper-Symonds model
parameters SRC and SRP in MAT_003 model, set equal to 255.4 and 7.6, respectively [10].

3.3 Loading, Boundary Conditions, and Contacts

The loading in this FE analysis is applied in the form of uniform initial velocity equal to
the impact velocity (V_i) at all nodes of the impact head (Figure 2). A constant downward
acceleration due to gravity, g, is applied at all nodes of the entire model to simulate gravity.

The external boundary conditions are applied at the base support, and the symmetry boundary conditions are applied at the x = 0 and y = 0 planes of the slab, as shown in Figure 2. The support is assumed to have no displacements (i.e. $u_x = u_y = u_z = 0$) at the bottom face. Due to symmetry about the x and y axes, the out of plane displacements and rotations are assumed zero at both x = 0 and y = 0 planes.

"Automatic surface-to-surface" contacts are employed in LS-Dyna for modeling the contact between the impact head and the slab as well as that between the slab and the support. Initially, at time = 0, the impact head is situated at 100 μm above the top face of the slab. The contacts are activated as soon as the falling impact head comes in contact with the slab. The significant input parameters, same for both contacts, are set as follows: static and dynamic coefficients of friction equal to 0.30 and 0.28, respectively; input card A is checked with soft constraint option set to 1; default values are used for all other parameters. The slab is considered as the 'slave' in both contacts (head-slab and support-slab).

4. SHCC MATERIAL MODEL

The concrete damage model MAT_072R3 of LS-Dyna material library, based on 3D concrete plasticity theory, is used in this research for modeling SHCC in the slab elements, following the work of Chin [10]. Although the MAT_072R3 model (also known as K&C model) was also originally developed by Malvar et al. [7] for concrete and tension-softening FRCs, it can be adopted for SHCC because it has (1) three separate fixed 'loading surfaces' (yield, ultimate, and residual), and (2) independent parameters for controlling the damage evolutions in tension and in compression. While the mathematical details of the MAT_072R3 model are presented in Malvar et al. [7] and other texts on concrete plasticity, the objective of this paper is to outline the main features and setup of this model so that all the inputs required for simulating an SHCC using the MAT_072R3 model can be correctly determined.

The input parameters for the MAT_072R3 material model in LS-Dyna can be broadly classified into three categories: (1) loading surfaces, (2) damage accumulation, and (3) other inputs. Each of these categories is discussed below, along with the determination of parameters for SHCC.

4.1 Loading Surfaces Parameters

Analogous to a stress-strain curve for uniaxial behaviour, a 3D failure surface as a function of the damage state of SHCC is used in MAT_072R3 to determine the material's deviatoric behaviour under multi-axial loads. As noted in Malvar et al. [7], the 3D failure surface in the post-elastic stage moves between three fixed 'loading surfaces', namely yield, maximum, and residual. Mathematically, at a particular damage state represented by damage parameter η in MAT_072R3, the failure surface is a linear combination of either the yield and the maximum or the maximum and the residual loading surfaces with coefficients η and (1-η).

Each of the three 3D loading surfaces is completely defined by a corresponding 2D loading curve (effective deviatoric stress capacity [$\Delta\sigma = \sqrt{3J_2}$] as a function of hydrostatic stress [p]), which is the intersection of the 3D loading surface and the compressive meridian plane in the Haigh-Westergaard stress-space. The eight parameters of MAT_072R3 grouped as: (a_{0y}, a_{1y}, a_{2y}), (a_0, a_1, a_2), and (a_{1f}, a_{2f}) describe the p-Δσ loading curves on the compressive meridian

of yield, maximum, and residual loading surfaces, respectively (expressions in first column of Table 1). A combination of uniaxial test results conducted by the authors and previous multi-axial tests on concretes with similar compressive strength are used as known data points (p, $\Delta\sigma$) to determine the eight parameters shown in Table 1.

Table 1: Loading surfaces input parameter determination for SHCC

Loading Surface	Description/ Data point Reference	p	$\Delta\sigma$ ($\sqrt{3J_2}$)	Parameter values for SHCC
Max, $\Delta\sigma_m =$ $a_0 + \dfrac{p}{a_1 + a_2 p}$	Uniaxial Compression/ Ref: [11]	$f_c'/3$	f_c' (160 MPa)	$a_0 = 24.10^6$ MPa $a_1 = 0.366$ $a_2 = 4.91.10^{-10}$ MPa^{-1}
	Pure shear in plane stress $(\sigma_1,\sigma_2,\sigma_3) = (f_{tm},0,-f_{tm})/$ Ref: Matrix cracking strength, f_{tm} [11]	0 MPa	$3f_{tm}$ (24 MPa)	
	Highly confined compression/ Ref: [12,13]	$4.6f_c'$	$6.5f_c'$	
Yield, $\Delta\sigma_y =$ $a_{0y} + \dfrac{p}{a_{1y} + a_{2y} p}$	Yield surface assumed as locus of points at $\Delta\sigma_y = 0.45\Delta\sigma_m$ on triaxial compression paths/ Ref: [7,14]	0 MPa	29.2 MPa	$a_{0y} = 22.6.10^6$ MPa $a_{1y} = 0.397$ $a_{2y} = 1.2.10^{-9}$ MPa^{-1}
		10 MPa	47.8 MPa	
		100 MPa	176.2 MPa	
Residual, $\Delta\sigma_r =$ $\dfrac{p}{a_{1f} + a_{2f} p}$	Brittle-ductile transition under triaxial compression assumed at p = $4f_c'$; intermediate point assumed at $2f_c'/$ Ref: [7,10]	$2f_c'$	$\Delta\sigma_m$ (p=2f_c'−f_{tm})	$a_{1f} = 0.356$
		$4f_c'$	$\Delta\sigma_m$ (p=4f_c')	$a_{2f} = 4.80.10^{-10}$ MPa^{-1}

4.2   Damage Accumulation Parameters

The damage parameter η (in Section 4.1) is defined as a function of cumulative effective plastic strain parameter, λ, in MAT_072R3. The parameter λ above is computed from the tensorial plastic strains, ε_{ij}^p, in the MAT_072R3 model using Eq. (1) [7]. The η-λ damage function is input by the user (Table 2) based on the shape of the material's experimental uniaxial compressive behaviour.

Table 2: Damage function η(λ)

λ	0	$1.2.$ 10^{-5}	$2.4.$ 10^{-5}	$4.$ 10^{-5}	$5.6.$ 10^{-5}	$7.2.$ 10^{-5}	$8.8.$ 10^{-5}	$1.0.$ 10^{-4}	$2.5.$ 10^{-4}	$7.0.$ 10^{-4}	$2.5.$ 10^{-3}	10	$1.0.$ 10^{10}
η	0	0.85	0.97	0.99	1	0.99	0.88	0.3	0.2	0.1	0	0	0

$$\lambda = \int_0^{\overline{\varepsilon^p}} \frac{d\overline{\varepsilon^p}}{r_f\left(1+{p}/{r_f f_t}\right)^{b_1}} \text{ for } p \geq 0 \text{ and } \lambda = \int_0^{\overline{\varepsilon^p}} \frac{d\overline{\varepsilon^p}}{r_f\left(1+{p}/{r_f f_t}\right)^{b_2}} \text{ for } p < 0, where \ d\overline{\varepsilon^p} = \sqrt{\frac{2}{3}\varepsilon_{ij}^p\varepsilon_{ij}^p} \quad (1)$$

In Eq. (1), f_t is the ultimate tensile strength (14.5 MPa for the SHCC in this study); r_f is the rate factor; b_1 and b_2 are the damage scaling parameters, which independently control the rates ($d\lambda/d\overline{\varepsilon^p}$) of damage accumulation in λ for positive (compression) and negative (tension) pressures, respectively – this is a unique feature of the MAT_072R3 model, which enables its adaptation for strain-hardening materials.

The values of the damage scaling parameters b_1 and b_2 used for the SHCC in this study are determined by matching the computed stress-strain responses of a single element with the experimental curves, and are set equal to -0.55 and -20, respectively. In the MAT_072R3 model, another damage scaling parameter b_3, in addition to b_1 and b_2, is used for tackling spurious results for triaxial tensile loading. Such loading is not expected in the modeled problem, and therefore, in absence of experimental data, the default value of 1.1 is used.

4.3   Other Parameters

Other parameters required as inputs in the MAT_072R3 model are density (2400 kg/m^3), Poisson ratio (0.20), and localization width of the crack (LOCWIDTH = 2 mm). LOCWIDTH is assumed equal to the element size, which is 2 mm, to prevent localization instabilities and spurious mesh sensitivity. Decreasing LOCWIDTH increases the observed ductility in both tension and compression.

4.4   Equation of State, Rate Effects, and Material Erosion

All the model parameters discussed thus far for defining the failure surface capture only the *deviatoric* behaviour of the material, and therefore, an 'equation of state' (EOS), which defines the *hydrostatic* behaviour of a material by relating the hydrostatic pressure to the volumetric strain, is needed to completely describe the material behaviour. For this purpose, the EOS of type 8 (EOS 8) in LS-Dyna, which inputs tabulated pressure-volumetric strain data points (linear variation is assumed between the specified points) along with instantaneous bulk modulus at these points (for unloading), is used. The temperature dependent variation of hydrostatic pressure is neglected in this study. The equation of state used for SHCC is automatically generated by LS-Dyna for similar compressive strength concrete, assuming the same hydrostatic compressive behaviour.

The rate effect on the material strength is incorporated in the model by specifying a 'load curve' in LS-Dyna, by relating dynamic increase factors (DIF) to strain rate. While the tensile DIFs are based on the experimental investigation by the authors [15], the compressive DIFs are based on past studies on similar high strength concretes. The rate effect on material's tensile ductility cannot be explicitly specified in LS-Dyna. Instead, the damage scaling parameters b_1 and b_2, along with the erosion criterion (given below) are chosen to simulate the material's ductility at the highest strain rate expected in the modeled problem (as the ductility of SHCC used in this study slightly decreases with strain rate).

Failure of the material is defined using tensile and compressive erosion criteria in this study. The erosion criterion (using MAT_ADD_EROSION keyword) for tensile strain is set at 2.9%, and that for hydrostatic pressure is set at 400 MPa.

Using the above parameters, the observed uniaxial stress-strain curves of the SHCC are satisfactorily modeled at various strain rates; for details, the reader is referred to Ranade [15].

5.   RESULTS AND DISCUSSION

In Figure 3, the force-time history computed from the FE analysis (FEA), for the impact on an SHCC slab with drop-weight of 16 kg and impact velocity of 4.6 m/s, is compared to the experimentally determined force-time history of the corresponding drop-weight impact. The computed curve (dashed) seems to have sharper contrast, with stronger peaks and valleys of the contact force with time, compared to the experimental curve. This may be caused due to limited sampling frequency (200 kHz per sensor) of the data acquisition (DAQ) system used in the drop-weight experiments. There is also a significant difference between the experimental and FEA computed peak contact force (PCF). In addition to the limited sampling frequency of the DAQ, this may also be caused by the influence of the surface texture of the slab in slightly slowing down the drop-weight assembly, before the impact head starts compressing the bulk of the material. In spite of this discrepancy, the computationally determined response shows a good agreement, overall, with the experimental force-time history, as the area under the force-time curve is approximately the same for both the curves.
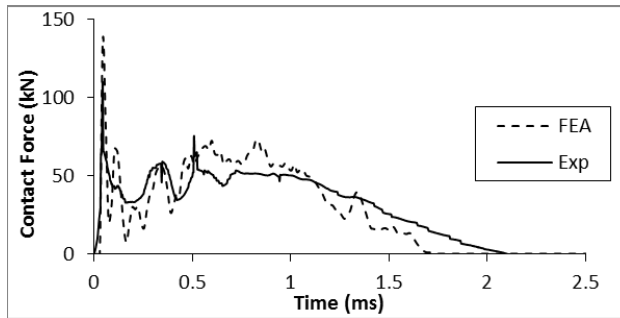
Figure 3: Contact force-time history comparison between experiment and FEA results

The PCF, along with the maximum mid-point displacement of the SHCC slab, determined from FE analysis for the three load cases (corresponding to three impact velocities) investigated in this study, are compared with the drop-weight experiment results in Table 3. As discussed above, the computationally determined PCF's are significantly higher than the experimentally observed PCF's. In contrast, the maximum displacements computed from the FE analysis closely match the maximum displacements derived from the observed acceleration time histories. The error in displacement estimation is less than 10% for all the load cases investigated in this study. The limitation of the sampling frequency is overcome in displacement computation by the integration of acceleration-time history, resulting in a better agreement between the experimental observations and FE analysis.

Table 3: Comparison of FE analysis with experimental results

Impact Velocity (m/s)	Peak Contact Force (kN)			Maximum Displacement (mm)		
	FEA	Exp.	Error (wrt Exp.)	FEA	Exp.	Error (wrt Exp.)
2.30	100	57	75.4%	1.04	1.15	-9.6%
3.25	121	77	57.1%	1.64	1.66	-1.2%
4.60	146	103	41.7%	2.59	2.78	-6.8%

In addition to above results, the FE analysis provides useful insights into the damage mechanisms and stress and strain profiles of the slab as functions of time. These insights and further details of the FE modelling are given in Ranade [15].

6.   CONCLUSIONS AND FUTURE WORK

The behaviour of an ultra-high strength SHCC was satisfactorily simulated using the MAT_072R3 material model in LS-Dyna, and verified through drop-weight experiment results. Although there is a discrepancy in the computed peak impact force as compared to the experimental results, the properties involving time-integration, such as displacement and area under the force-time curve (impulse), showed good agreement with the experimental results.

In spite of the satisfactory modelling of SHCC in this preliminary study, MAT_072R3 has certain limitations, such as lack of strain rate sensitivity to material's ductility, which will have to be addressed in the future. The feasibility of modelling SHCC under cyclic loading, such as under earthquakes, using the MAT_072R3 is also unknown. Addressing these limitations, among others, may lead to a new material model in the LS-Dyna library developed explicitly for modelling SHCC under dynamic loads.

REFERENCES

[1] Chen, W.F., Plasticity in Reinforced Concrete. (1982) 190-294.
[2] Kabele, P., Analytical modeling and fracture analysis of engineered cementitious composites. PhD thesis, The University of Tokyo (1995).
[3] Boshoff, W.P. and van Zijl, G.P.A.G., 'A computational model for strain-hardening fibre-reinforced cement-based composites', Journal of S. Afr. Inst. Civ. Eng. 49 (2007) 24–31.
[4] Dick-Nielsen, L., Modeling of ECC materials using numerical formulations based on plasticity. Ph.D. thesis, Technical University of Denmark (2008).
[5] Suryanto, B., Nagai, K. and Maekawa, K., 'Modeling and analysis of shear-critical ECC members with anisotropic stress and strain fields', J. Adv. Concr. Technol. 8 (2010) 239–258.
[6] Rokugo, K. and Kanda, T., 'Strain Hardening Cement Composites: Structural Design and Performance', State-of-the-art report of the RILEM Technical Committee 208-HFC, SC3, (2013).
[7] Malvar, L.J., Crawford, J.E., Wesevich, J.W. and Simons, D., 'A plasticity concrete material model for DYNA3D' *International Journal of Impact Engineering*. 19 (9-10) (1997) 847-873.
[8] Schwer, L.E., 'Preliminary Assessment of Non-Lagrangian Methods for Penetration Simulation', in Proc. of 8th International LS-DYNA User Conference, Dearborn, MI, May, 2004 pp.8.
[9] Agardh, L. and Laine L., '3D FE-Simulation of High-Velocity Fragment Perforation of Reinforced Concrete Slabs', *International Journal of Impact Engineering*. 22 (9-10) (1999) 911-922.
[10] Chin, L.S., Finite Element Modeling of Hybrid-Fiber ECC Targets Subjected to Impact and Blast, PhD thesis, National University of Singapore (2006).
[11] Ranade, R., Li, V. C., Stults, M. D., Heard, W. F. and Rushing, T. S., 'Composite Properties of High-Strength, High-Ductility Concrete', *ACI Materials Journal*. 110 (4) (2013) 413-422.
[12] Girgin, Z.C., Arioglu, N. and Arioglu, E., 'Evaluation of Strength Criteria for Very-High-Strength Concretes under Triaxial Compression', *ACI Structural Journal*. 104 (3) (2007) 277-283.
[13] Attard, M.M. and Setunge, S., 'Stress-Strain Relationship of Confined and Unconfined Concrete', *ACI Materials Journal*. 93(5) (1996), 432-442.
[14] Joy, S. and Moxley, R., 'Material Characterization, WSMR-5 ¾″ Concrete', Report to the Defense Special Weapons Agency, USAE Waterways Experiment Station, Vicksburg, MS (1993).
[15] Ranade, R., Advanced Cementitious Composite Development for Resilient and Sustainable Infrastructure, PhD thesis, University of Michigan Ann Arbor (2014).